

ES Energy & Environment

DOI: https://dx.doi.org/10.30919/esee8c653



Anomalous Thermal Conductivity Induced by High Dispersive Optical Phonons in Rubidium and Cesium Halides

Zheng Chang, ¹ Kunpeng Yuan, ¹ Jiale Li, ² Zhehao Sun, ³ Jiongzhi Zheng, ⁴ Mohammed Al-Fahdi, ⁵ Yufei Gao, ¹ Bin Wei, ^{2,*} Xiaoliang Zhang, ^{1,*} Ming Hu^{5,*} and Dawei Tang^{1,*}

Abstract

Knowledge of lattice dynamics is essential for understanding the physical properties of materials and optimizing the performance for applications. Alkali halides (MX, M=Na, K, Rb, and Cs; X=Cl, Br, and I) have been widely recognized for their simple crystal structures and low thermal conductivities. At room temperature, the thermal conductivity (κ) of RbBr is nearly twice as large as that of RbCl and RbI, while the thermal conductivities of three compounds in CsX halides are comparable. These thermal conductivity trends with increased atomic mass are significantly different from the common sense that the thermal conductivity conventionally decreases with the increasing atomic mass and decreasing electronegativity difference. However, little attention has been paid to the microscopic mechanism of these anomalous thermal conductions in RbX and CsX. Here, we report a systematic investigation of the thermal transport properties in alkali halides by the Boltzmann transport equation based on first-principles calculations. The results show that the anomalous thermal conductivity trends of RbX and CsX mainly attribute to the disparity of optical phonons in each compound. The more dispersive the optical phonons, the greater their contribution to the thermal conductivity, and thus the thermal conductivities of compounds with heavier atoms are enhanced. The disparity of optical phonons originates from the mass difference in the compound. Our work offers deeper insight into the unusual phonon thermal transport phenomenon in alkali halides, and provides fundamental reference for rooting the thermal conductivities in related functional materials and finding novel materials with thermal conduction beyond the conventional cognition.

Keywords: Abnormal thermal transport; Lattice thermal conductivity; Alkali halides; Phonon dispersion; Boltzmann transport equation.

Received: 03 January 2021; 30 January 2022; Accepted: 14 February 2022.

Article type: Research article.

1. Introduction

Alkali halides are widely utilized in new opto-electronic devices due to fascinating electro-optic properties,^[1] electro-mechanical properties,^[2] and large electronegativity and dielectric constants.^[3] These prominent properties associate closely with phonon thermal transport properties, such as lattice vibrations ^[4-5] and thermal conductivities.^[6-7] For most compounds in alkali halides, the thermal conductivities are

relatively low, and the values at room temperature range from 1 to 7 W/mK.^[8] Previous works have been performed to investigate the thermal properties of alkali halides using classical theoretical methods.^[8-11] However, the underlying mechanism of such low thermal conductivity has not been fully understood. Modern computational techniques have been successfully utilized to probe novel physical behaviors, such as negative thermal expansion.^[12] anisotropic thermal conduction,^[13-14] and ultralow thermal conductivity.^[15-17] Recent theoretical reports mainly take alkali halides as models to verify the accuracy of the improved prediction of thermal conductivity,^[18-19] but the inherent thermal transport of alkali halides is rarely concerned.^[7,20-22] Therefore, a systemic revisit to the thermal transport properties in alkali halides by state-of-art computational techniques is of urgent necessity.

According to Slack's theory,^[23] four factors are needed for low thermal conductivity: (1) large atomic mass, (2) weak bonding, (3) complex crystal structure, and (4) strong

¹ Key Laboratory of Ocean Energy Utilization and Energy Conservation of Ministry of Education, School of Energy and Power Engineering, Dalian University of Technology, Dalian 116024, China.

² Henan Key Laboratory of Materials on Deep-Earth Engineering, School of Materials Science and Engineering, Henan Polytechnic University, Jiaozuo 454000, China.

³ Research School of Chemistry, Australian National University, Canberra, ACT 2601, Australia.

Research article ES Energy & Environment

anharmonicity. Recently, Lindsay et al reported that large phonon bandgaps, low Debye temperature, and the acoustic bunching will also induce low thermal conductivity. [24-25] These effects have been successfully utilized to reveal the ultrahigh thermal conductivities in BAs^[26] and θ -TaN.^[27] However, Alkali halides possess relatively simple crystal structures (face-centered and simple cubic structures) with ionic bonds, which are usually unexpected to hold low thermal conductivity. Generally, the thermal conductivity decreases with the increasing atomic mass and the electronegativity difference. [23-^{24,28]} In alkali halides, NaX and KX hold the thermal conductivities following this common routine well from MCl to MI ($\kappa_{\text{NaCl}} > \kappa_{\text{NaBr}} > \kappa_{\text{NaI}}$ and $\kappa_{\text{KCl}} > \kappa_{\text{KBr}} > \kappa_{\text{KI}}$), but it is not the case for RbX and CsX. In these two systems, RbBr holds a larger thermal conductivity than RbCl and RbI, and CsX halides hold comparable lattice thermal conductivities for each compound.[8,29-30] In particular, a novel phonon heat conduction mechanism (Phonon Coherence)[31-32] may unveil the origin of abnormal κ trends in MX compounds, which takes into account phonon as a vibrational wave not the conventional phonon gas model. Such the unusual behaviors are significantly unconventional and are difficult to understand by the theories introduced above. Thus, a further investigation of the structure, bond features, and thermal transport is of urgent need to elucidate the origin of these anomalous thermal conductivity trends in RbX and CsX.

In this paper, the abnormal phonon thermal transport mechanism in alkali halides is fully explored by using the Boltzmann transport equation based on density functional theory. Our calculated results are in good consistence with previous experiments. In NaX and KX, the thermal conductivity decreases with increasing atomic mass, which follows the conventional theories well. The anomalous thermal conductivity trends in RbX and CsX are revealed, which attributes to the dispersive optical phonons, contributing more on the thermal conductivity in the compounds with heavier atomic mass. The disparity originates from the atomic mass difference, i.e., the larger the mass difference is, the more dispersive branch the optical phonon behaves. This work offers a microscopic insight into anomalous phonon transport mechanisms in alkali halides and provides a fundamental guidance for other related systems with unconventional low thermal conductivity trends, which could further aid the design of functional materials.

2. Computational methods

All the calculation are performed by using the projector-

augmented-wave (PAW)[33] potentials as implemented in the Vienna Ab Initio Simulation Package (VASP)[34-35] within the framework of density functional theory (DFT).[36] The device studio[37] program was used for visualization and modeling. The local density approximation (LDA) functional was used for exchange-correlation functional and the energy cutoff of plane-wave basis was set as 550 eV. Monkhorst-Pack k-mesh of 8×8×8 was applied to sample the irreducible first Brillouin zone (BZ), and the energy convergence threshold was set as 10⁻⁸ eV for structural optimization. The all-primitive cells in the work were fully optimized and all atoms were allowed to relax until the maximal Hellmann-Feynman force acting on each atom was no longer than 10⁻⁶ eV/Å. The bonding mechanism of different NaCl- and CsCl-type structures was investigated using the standalone computer program Local Suite Electronic-Structure Orbital **Basis** towards Reconstruction (LOBSTER).[38] Meanwhile, the strength of ionic bonding is reflected by the mechanical characteristics of materials. To deeply examine the mechanical stability of the selected compounds, we calculated the elastic constants, as shown in Table S1 in the supplementary information. Densityderived electrostatic and chemical (DDEC6) method using the packages named CHARGEMOL^[39-41] is used to calculate the transferred and shared charges. The transferred electrons are directly extracted from the net atomic charges file outputted by CHARGEMOL package. The delocalization indices are extracted from the file of overlap populations. The shared charges are twice the delocalization index. Therefore, the values extracted from the overlap populations are multiplied by two to obtain the shared electrons in the materials.

The second-order interatomic force constants (IFCs) and third-order IFCs were calculated by Phonopy^[42] and ShengBTE codes^[43] using a $4\times4\times4$ supercell (containing 128 atoms) and $2\times2\times2$ **k**-grid in the BZ, further obtaining the related phonon properties and thermal conductivity. In addition, the Born effective charge and dielectric constant were computed to correct the dynamical matrix for considering long-ranged electrostatic interactions based on density functional perturbation theory (DFPT).^[44] After our convergence test, the cutoff distance of anharmonic IFCs for the above compounds is set as the 9th nearest neighbor. Meanwhile, the κ convergence of NaCl and CsCl crystals with respect to the q-mesh has been calculated and plotted in Fig. S1 in the supplementary information.

3. Results and discussions

Alkali halides are affiliated with the face-centered cubic (NaCl-type, NaX, KX, and RbX) and simple cubic (CsCl-type, CsX) crystal structures (Fig. 1e). Fully relaxed lattice constants and bond lengths of each compound agree well with experimental values, [45] as listed in Table 1. Figs. 1a-d show the calculated temperature-dependent thermal conductivity of all studied compounds. Our calculations almost show good agreement with previous measurements [8,30] (Detailed comparison is listed in Table S2). It is worth noticing that the

⁴ Department of Mechanical and Aerospace Engineering, The Hong Kong University of Science and Technology, Clear Water Bay, Kowloon, Hong Kong 999077, China.

⁵ Department of Mechanical Engineering, University of South Carolina, Columbia, South Carolina 29208, USA.

^{*}Email: binwei@hpu.edu.cn (B. Wei), zhangxiaoliang@dlut.edu.cn (X. Zhang), hu@sc.edu (M. Hu), dwtang@dlut.edu.cn (D. Tang)

ES Energy & Environment Research article

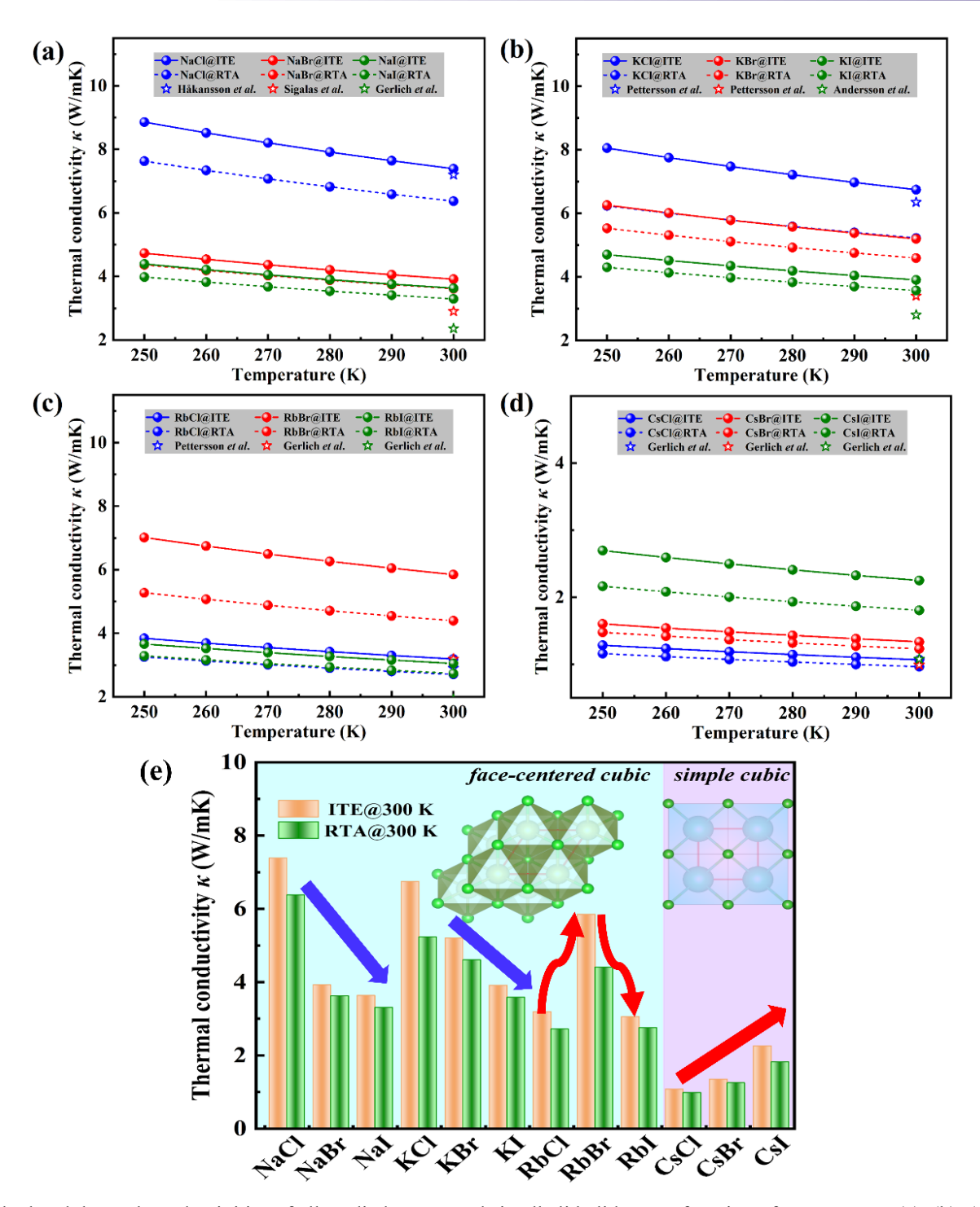


Fig. 1 Calculated thermal conductivities of all studied compounds in alkali halides as a function of temperature. (a), (b), (c), and (d) are the relaxation time approximation (RTA) and iteratively solving (ITE) results for NaX (X=Cl, Br, and I), KX (X=Cl, Br, and I), RbX (X=Cl, Br, and I), and CsX (X=Cl, Br and I), respectively, compared with previous measurements. Reproduced with permission from [8], [47], [48] and [49]. Copyrights@IOP Publishing and @Spring Publishing. (e) Comparison of the thermal conductivities in alkali halides at 300 K. Arrows indicate the thermal conductivity trend with increasing atomic mass in each system.

relaxation time approximation (RTA) results are lower compared to the iteratively solving (ITE) results because the normal scattering processes is also taken into account by RTA when blocking the heat transport, [46] suggesting the dominant role of the Umklapp processes in thermal conduction from 250 K to 300 K. It is clearly seen that κ_{NaCl} calculated by the RTA in Fig. 1a is largely deviated from the ITE results, while κ_{NaBr}

and κ_{NaI} are nearly the same. Therefore, in materials such as NaCl, NaBr and NaI, the Umklapp scattering of the latter two is stronger so the behavior of κ is mainly determined in this Umklapp scattering processes. For comparison, the values of thermal conductivity of each compound at 300 K are shown in Fig. 1e. It is obviously shown that the thermal conductivity exhibits decreasing trend from MCl to MI in NaX and KX

Research article ES Energy & Environment

Table 1. Calculated average atomic mass (m_{avg}) , mass difference (m_{diff}) , primitive cell lattice constant (a), bonding length (l) and strength (Crystal orbital Hamilton population, COHP), a-o gap, electronegativity difference (χ_{diff}) , acoustic and optical phonon contribution to thermal conductivity $(a_{\kappa}$ and $o_{\kappa})$, and Debye temperature (θ_{D}) for the selected alkali halide crystals. The ICOHP value is assumed to be the additive inverse of the integral of a "-COHP" curve to the whole energy range.

MX	a (Å)	l(Å)	ICOHP (meV)	$m_{\rm avg}$ (amu)	$m_{\rm diff}$ (amu)	gap (THz)	χdiff	a_{κ} %	O _K %	$\theta_{\mathrm{D}}\left(\mathrm{K}\right)$
NaCl	3.84	2.85	-5.37	29.22	12.46	_	2.1	85.36	14.64	280.92
NaBr	4.07	3.01	-3.48	51.45	56.91	0.796	1.9	93.37	6.63	193.48
NaI	4.41	3.27	-1.70	74.95	103.91	1.308	1.6	96.76	3.24	142.65
KC1	4.33	3.20	-2.82	37.28	3.65	_	2.2	75.20	24.80	223.49
KBr	4.54	3.36	-2.51	59.50	40.81	0.417	2.0	92.35	7.65	162.10
KI	4.85	3.59	-1.51	83.00	87.80	0.966	1.7	96.47	3.53	121.60
RbCl	4.54	3.35	-3.37	60.46	50.02	0.436	2.2	94.56	5.44	165.60
RbBr	4.74	3.51	-4.67	82.69	5.56	_	2.0	80.50	19.50	130.09
RbI	5.05	3.74	-5.91	106.19	41.43	_	1.7	90.16	9.84	103.20
CsCl	3.98	3.65	-238.61	84.18	97.46	0.302	2.3	89.08	10.92	120.35
CsBr	4.15	3.80	-281.40	106.40	53.00	_	2.1	84.25	15.75	102.61
CsI	4.41	4.04	-304.51	129.90	6.01	_	1.8	67.15	32.85	88.55

 $(\kappa_{NaCl} > \kappa_{NaBr} > \kappa_{NaI}$ and $\kappa_{KCl} > \kappa_{KBr} > \kappa_{Kl}$), which is in accordance with the common knowledge (thermal conductivity generally decreases with increasing atomic mass) mentioned above. Surprisingly, the thermal conductivity of RbBr is higher than that of RbCl and RbI ($\kappa_{RbBr} > \kappa_{RbCl} > \kappa_{RbI}$), and the thermal conductivities in CsX are comparable with a little increase trend from CsCl to CsI ($\kappa_{CsI} > \kappa_{CsBr} > \kappa_{CsCl}$), although the atomic mass of the two systems gradually increased from MCl to MI compounds.

In most insulators and semiconductors, thermal conductivity is mainly dominated by phonons, which determine the two primary factors: phonon group velocity and scattering rate, in the following equation:

$$\kappa_{\alpha\beta} = \frac{1}{3} \sum_{\lambda} c_{\lambda} \, v_{\lambda}^{\alpha} \, v_{\lambda}^{\beta} \tau_{\lambda} \tag{1}$$

where c_{λ} is the specific heat capacity of phonon mode λ , $v_{\lambda}^{\alpha(\beta)}$ is the group velocity of phonon mode λ along the α (β) direction, and τ_{λ} is relaxation time of phonon mode λ . To explore the anomalous thermal conductivities in RbX and CsX, the phonon properties should be systemically investigated. Fig. 2 shows the calculated phonon dispersions for all studied compounds, which agree well with available experimental data. [7,29,47-56] The general shape of phonon dispersions in NaCltype (Figs. 2a-i) and CsCl-type (Figs. 2j-l) compounds look vastly similar. Intuitively, there exists some phonon band gap between the acoustic (a) and optical (o) phonon branches in specific NaCl-type (~0.796 THz for NaBr, ~1.308 THz for NaI, \sim 0.417 THz for KBr, \sim 0.966 THz for KI, and \sim 0.436 THz for RbCl) and CsCl-type structures (~0.302 THz for CsCl) due to larger atomic mass difference. They won't give significant impact on the three-phonon scattering processes because the a-o gaps are not large enough to limit the aao (acoustic + acoustic → optical) phonon scattering process.^[57-58] Such effect is revealed by the comparable phonon lifetime of each compound (Fig. S2), which inversely related to the scattering rate, indicating the little impact of the a-o gap on the scattering process.

The related bond information (COHP in Fig. S3 and electronic band structures in Fig. S4) and the θ_D were also calculated (Detailed calculation can be found in Note S1) to recognize the main factors that cause the unconventional thermal conductivity trends in RbX and CsX, as listed in Table with average atomic mass, mass difference, electronegativity difference, lattice constant, bond length, a-o gap, acoustic and optical contributions to thermal conductivity. It can be found that as the atomic number increased, the atomic mass, lattice constant, and bond length are all increased, while the electronegativity difference and the θ_D are decreased for each system. It is well known that a lower θ_D means the smaller phonon velocities and average lower phonon frequencies, and a lower-frequency phonons further rise phonon populations, leading to the increase of three-phonon scattering rates. These factors, including the bond strength (ICOHP), perfectly follow the conventional theory and agree well with the thermal conductivity trends in NaX and KX but are not applicative in RbX and CsX. For other factors, it is interesting that both the change of the a-o gap and optical phonon contribution to thermal conductivity are closely related to the change of mass difference. To further analyze and quantify the unusual behavior, we calculated the shared and transferred charges for the selected alkali halide compounds in which the anomalous lattice thermal conductivities occur (Detailed analysis in the supplementary information), as illustrated in Table S3. Meanwhile, we present calculations of the κ and related to phonon properties for selected alkali halides, including threephonon scattering processes, Grüneisen parameter and the m_{avg} effect, as depicted in Fig. S5.

Meanwhile, the cumulative phonon density of states (PDOS) and weighted phase space (W) are plotted in Fig. S6. It can be easily observed that the cumulative PDOS of RbI (CsI) are generally larger than that of RbCl (CsCl) by a factor 1.65 and 1.82 respectively, which are more evident for PDOS. The increased factors manifest the influence of the high-frequency optical phonons for the thermal transport process.

ES Energy & Environment Research article

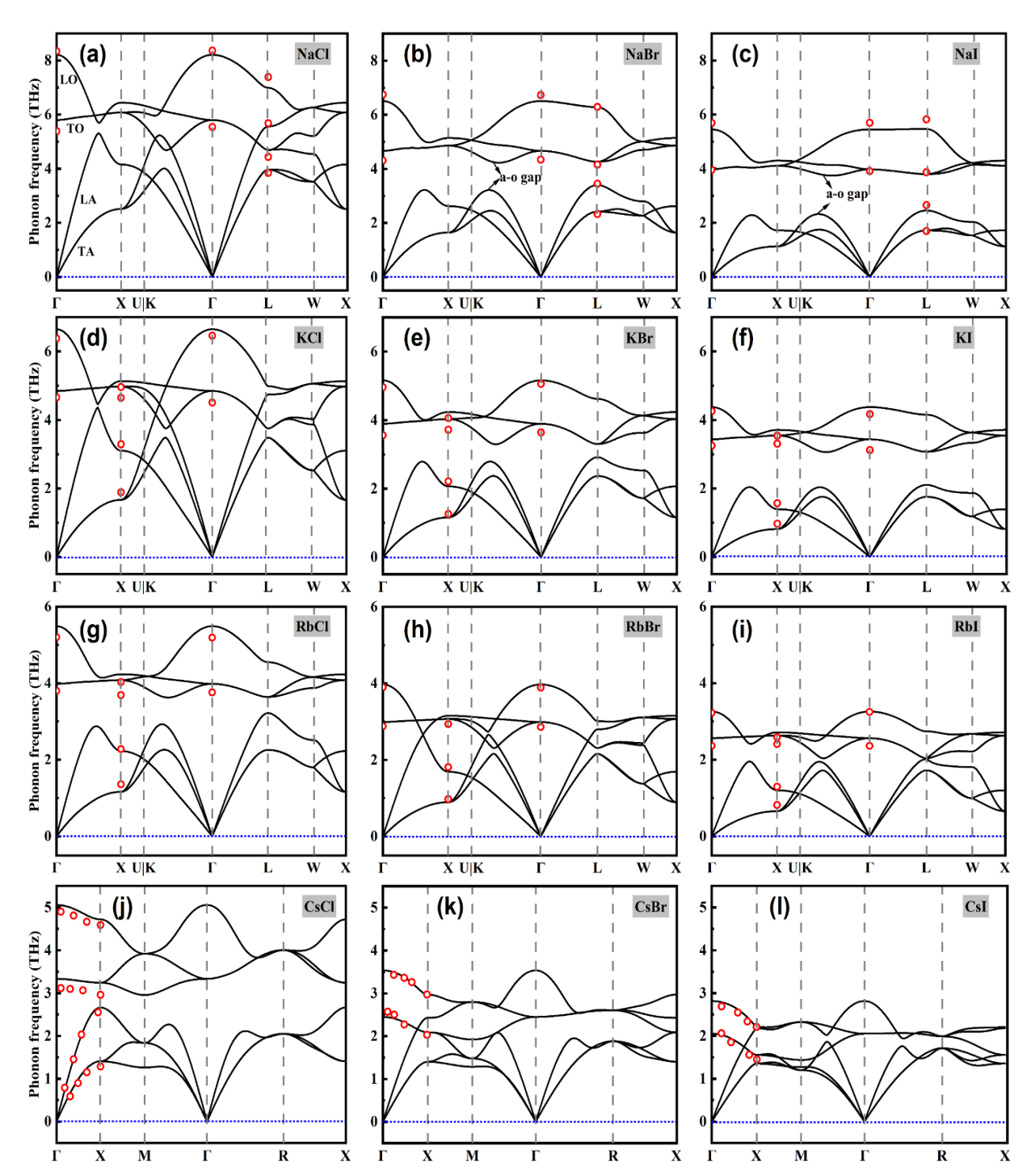


Fig. 2 Phonon dispersions for all studied compounds, compared with available experimental data. (a-l) are the dispersion curves of NaCl, NaBr, NaI, KCl, KBr, KI, RbCl, RbBr, RbI, CsCl, CsBr, and CsI, respectively. Reproduced with permission from [7], [29], [47] and [56]. Copyright@American Physical Society.

Thus, an apparent gradual increase of W in RbI (CsI) is expected. Obviously, we also observed that the W of RbX and CsX compounds are similar in shape and magnitude. In CsX, W for CsI is much larger, expected to be the cause of its increased phonon scattering. Surprisingly, these results are not consistent with phonon lifetime data as illustrated in Figs. S2(c-d). Thus, we can conclude that the scattering rates are roughly proportional to W, and it can mainly depend on the atomic mass difference for some materials due to a relatively

heavier atom resulting in smaller atomic displacement further suppressed the scattering.

The *a-o* gap increases with the increased mass difference, while the optical phonon contribution to thermal conductivity increases with the decreased mass difference. As discussed above, the *a-o* gap has little impact on the thermal conductivity due to the comparable scattering rates in RbX and CsX. Therefore, the abnormal thermal conductivity trends in these two systems can be traced to the optical phonons. Fig. 3 shows

Research article ES Energy & Environment

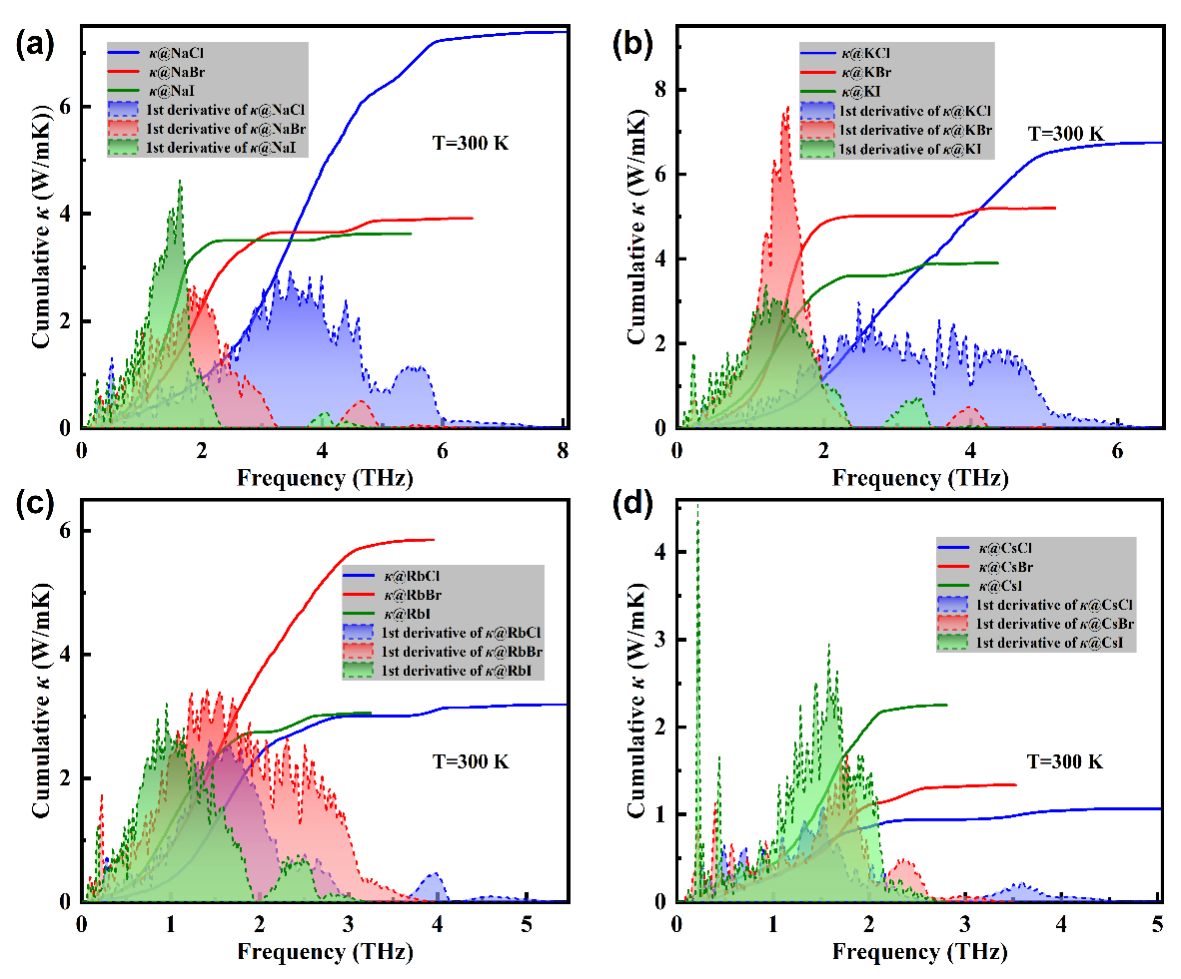


Fig. 3 Calculated phonon frequency-dependent cumulative thermal conductivity and their derivatives with respect to the frequency. (a), (b), (c), and (d) are results for NaX (X=Cl, Br and I), KX (X=Cl, Br and I), RbX (X=Cl, Br and I), and CsX (X=Cl, Br and I), respectively. The different dotted areas are the first-order derivatives of thermal conductivities for all studied compounds with respect to the frequency.

the calculated frequency-dependent cumulative thermal conductivity and their derivatives with respect to the frequency for the studied compounds. It is obviously shown that in the compounds with small mass difference (NaCl, KCl, RbBr, and CsI), the peak areas (frequency contribution) are more continuous with no gaps and have larger value than those in other compounds in the higher frequency region. Such higher peak height represents the optical phonon contribution, which plays a significant role in thermal transport in NaCl, KCl, RbBr, and CsI.

As shown in Fig. 4, the optical phonons possess larger group velocities in these compounds, which cause the larger thermal conductivities, and thus the unconventional thermal conductivity trend with increasing atomic masses in RbBr and CsI. It should be noted that the thermal conductivity trend in NaX (KX) is seemingly consistent with the traditional theory because the small mass difference between Na (K) and Cl (Cl) induces the largest optical phonon group velocity of NaCl (KCl), making the largest thermal conductivity for NaCl (KCl), similar for NaBr (KBr) and NaI (KI). As is known, the steepness of a phonon branch determines the value of its group velocity, i.e., the flatter the branch is, the smaller the group average mass is increased, and thus the group velocity

velocity it holds. Obviously, the longitudinal optical (LO) branch (the highest frequency mode around Γ point in the phonon dispersion) behaves as the more dispersive branch in NaCl, KCl, RbBr, and CsI, compared to the other two transverse optical (TO) branches. Thus, finding out the relationship between the dispersity of the phonon branches, especially for the LO branch, and the mass difference is the key to explore the origin of the high thermal conductivity in compounds with small mass difference or the anomalous thermal conductivity trend in RbX and CsX.

Due to the adopted cubic structure of alkali halides, the dispersity of phonon branches can be briefly described by the classical one-dimensional harmonic diatomic chain model with the nearest neighbours combined by identical springs with elastic constant β . Here, we take RbX as an example to reveal the origin of the dispersive behavior of the longitudinal acoustic (LA) and LO branches modulated by the mass difference. As shown in Fig. 5, the frequency of LA at zone boundary (π/a) decreases slightly from the model with $m_1 >$ m_2 to the model with $m_1 < m_2$, because the β will be enhanced by the stronger bond strength to some extent although the

Research article ES Energy & Environment

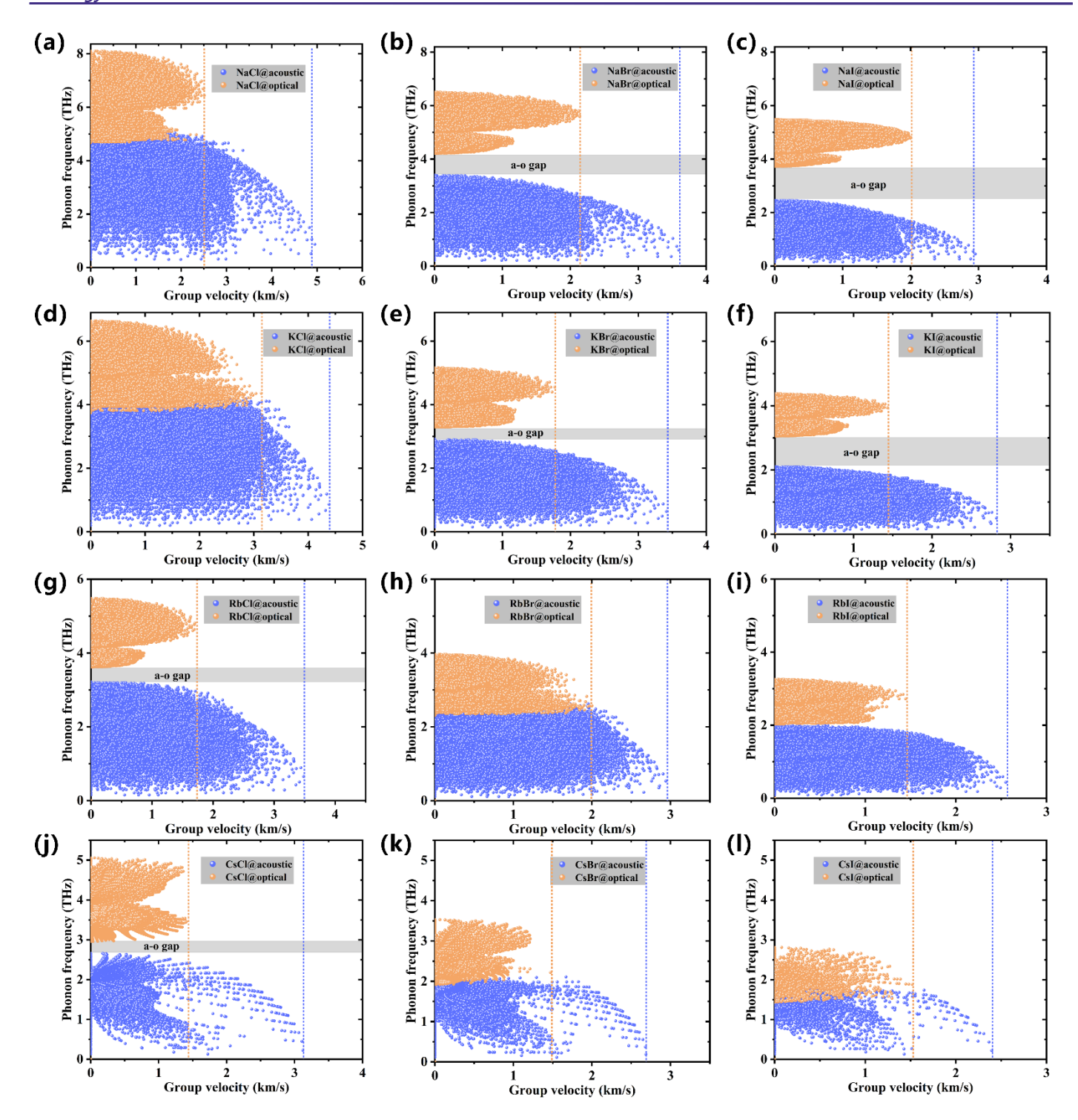


Fig. 4 Calculated acoustic and optical phonon group velocities for studied compounds. (a-l) are the results for NaCl, NaBr, NaI, KCl, KBr, KI, RbCl, RbBr, RbI, CsCl, CsBr, and CsI, respectively. The orange and blue dotted lines represent the largest group velocity of the acoustic and optical phonons, respectively.

decreases slightly from Fig. 5b to Fig. 5d (Figs. 4g-i). For the CsX, due to the increased bond strength from CsCl to CsI, the LO branch, the difference between the frequency at zone boundary and that at zone center is larger in the model with m_1 = m_2 than in the models with $m_1 > m_2$ and $m_1 < m_2$ due to the smallest atomic mass difference, which provides larger group velocity in Fig. 5c than in Fig. 5b and Fig. 5d (Figs. 4g-i), making the highest thermal conductivity in Fig. 5c (Fig. 1e). This model can also be analogized to CsX and Na(K)X. In strength from Na(K)Cl to Na(K)I, the LA group velocity

LA group velocity also decreases slightly with a ratio of 0.77 (the largest acoustic velocity of MI over that of MCl) as the case in RbX with a ratio of 0.75. For the LO branch, the group velocity increases from CsCl to CsI due to the mass difference decreased, and thus the increased thermal conductivity in CsX from CsCl to CsI. In Na(K)X, due to the decreased bond Research article ES Energy & Environment

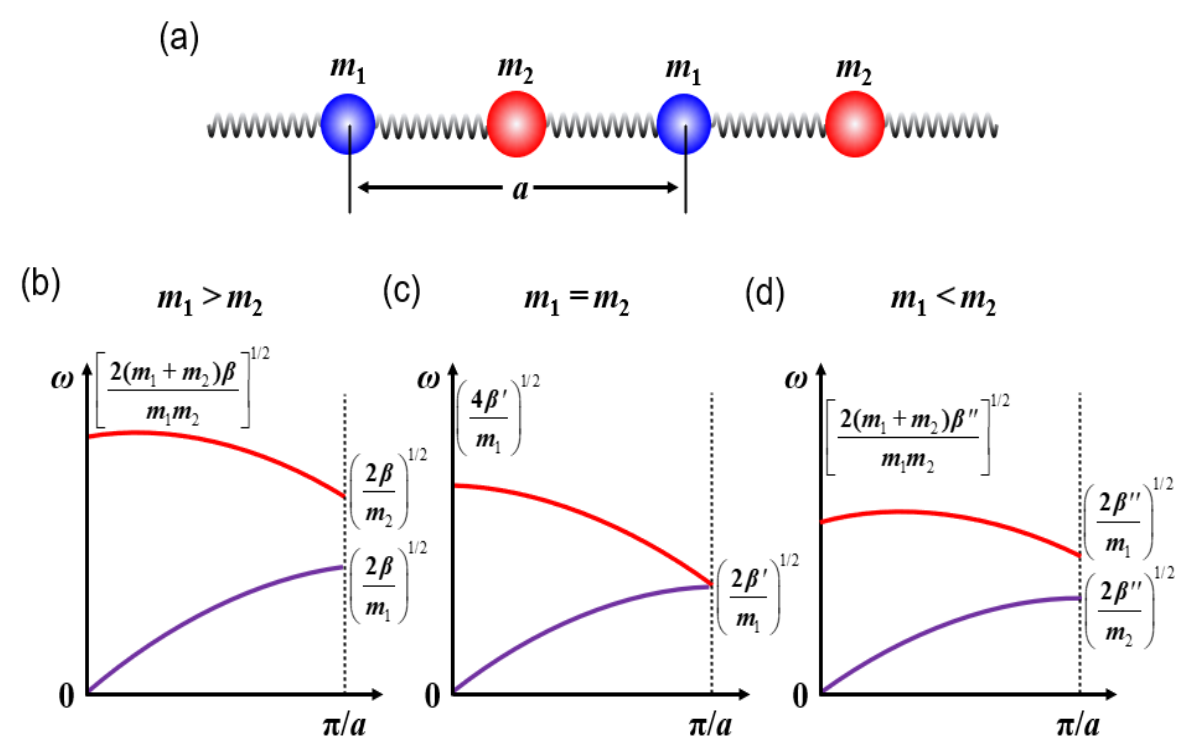


Fig. 5 Schematic change of phonon dispersion induced anomalous thermal conductivity trend in RbX. (a) one-dimensional harmonic diatom chain (lattice constant a, spring constant β , atomic mass m). (b), (c), and (d) are the related phonon dispersion with in the models with $m_1 > m_2$, $m_1 = m_2$, and $m_1 < m_2$, respectively. $(2\beta/m_1)^{1/2}$, $(2\beta'/m_1)^{1/2}$, and $(2\beta''/m_2)^{1/2}$ are the frequency of longitudinal acoustic phonon at zone boundary (π/a) . $[2(m_1+m_2)\beta/m_1m_2]^{1/2}$, $(4\beta'/m_1)^{1/2}$, and $[2(m_1+m_2)\beta''/m_1m_2]^{1/2}$ are the frequency of longitudinal optical phonon at zone center, while $(2\beta/m_2)^{1/2}$, $(2\beta'/m_1)^{1/2}$, and $(2\beta''/m_1)^{1/2}$ are the frequency of longitudinal optical phonon at zone boundary (π/a) .

strongly decreases with a ratio of 0.59 (0.65). For the LO branch, the group velocity decreases from Na(K)Cl to Na(K)I due to the mass difference increased, and thus the decreased thermal conductivity in Na(K)X from Na(K)Cl to Na(K)I structures.

As discussed above, the thermal conductivity trend difference between Na(K)X and Rb(Cs)X attributes to the bond strength and the mass difference. Recently, the interlayer rotation induced some changes in the bond strength and the mass difference was reported with tuning anomalous phonon behavior in a crystalline material. The former causes the larger decrease of the LA group velocity in Na(K)X than that in Rb(Cs)X, and the latter cause the larger LO group velocity in the compound with small mass difference. While in RbX and CsX compounds, due to the slightly decreased LA group velocity (having comparable impact on the κ), the anomalous thermal conductivity trend is mainly induced by the mass difference.

4. Conclusion

In summary, the thermal transport properties were systemically investigated in alkali halides by solving the Boltzmann thermal equation based on first-principles calculations. The origin of the anomalous thermal conductivity trend in RbX and CsX was revealed by the dispersity of the optical phonons. The smaller mass difference

the compound holds, the more dispersive the optical phonon behaves, and thus larger optical group velocity contributes to the thermal conductivity. Such result is applicable in all the studied systems in alkali halides, which is beyond the conventional theories. The present work revisits the thermodynamics of alkali halides by using the modern computing techniques, reveals the new underlying mechanism for the anomalous thermal conductivities in RbX and CsX. and paves new path to explore the microscopic origin for related systems with unconventional thermal conductivity trend.

Acknowledgements

This work is supported by the National Natural Science Foundation of China [51720105007, 52076031, 11602149, 51806031] and the Fundamental Research Funds for the Central Universities [DUT19RC(3)006], and the computing resources from the Supercomputer Center of Dalian University of Technology. The work at Henan Polytechnic University is supported by the Doctoral Foundation of Henan Polytechnic University (in Natural and Science) (NO. B2021-12) and the Fundamental Research Funds for the Universities of Henan Province (NO. NSFRF220421). B.W. was partially supported by the postgraduate research opportunities program of HZWTECH (HZWTECH-PROP). Research reported in this publication was supported in part by the NSF (award number 1905775, 2030128).

ES Energy & Environment Research article

Conflict of Interest

There is no conflict of interest.

Supporting Information

Applicable.

References

- [1] K. Subbaswamy, G. Mahan, *Phys. Rev. B*, 1985, **32**, 5453.
- [2] J. Schreuer, S. Haussühl, *J. Phys. D: Appl. Phys*, 1999, **32**, 1263.
- Kumar, C. K. Reddy, S. N. Ahmed, Opt. Mater., 2008, 31, 209-
- [4] R. H. Lyddane, R. Sachs, E. Teller, *Phys. Rev.*, 1941, **59**, 673-676.
- [5] M. Prange, L. Campbell, S. Kerisit, *Phys. Rev. B*, 2017, **96**, [36] W. Kohn, L. J. Sham, *Phys. Rev. B*, 1965, **140**, A1133. 104307.
- [6] M. Sist, K. F. F. Fischer, H. Kasai, B. B. Iversen, Angew. Chem., China, 2017, **129**, 3679-3683.
- [7] B. Wei, X. Yu, C. Yang, X. Rao, X. Wang, S. Chi, X. Sun, J. Hong, Phys. Rev. B, 2019, 99, 184301.
- [8] P. Andersson, J. Phys. C: Solid State Phys., 1985, 18, 3943.
- [9] R. A. Cowley, Anharmonic crystals. *Rep. Prog. Phys.*, 1968, 31, 123.
- [10] R. Cowley, W. Cochran, B. Brockhouse, A. Woods, *Phys*. Rev., 1963, 131, 1030.
- [11] S. Pettersson, *J. Phys. C: Solid State Phys.*, 1987, **20**, 1047.
- [12] C. W. Li, X. Tang, J. A. Munoz, J. B. Keith, S. J. Tracy, D. L. Abernathy, B. Fultz, *Phys. Rev. Lett.*, 2011, **107**, 195504.
- [13] B. Wei, Q. Cai, Q. Sun, Y. Su, A. H., Said, D. L. Abernathy, J. Hong, C., Li, *Commun. Phys.*, 2021, **4**,1-9.
- [14] B. Wei, J. Liu, Q. Cai, A. Alatas, M. Hu, C. Li, J., Hong, Rev. B, 2000, 61, 11425. Mater. Today Phys., 2022, 22, 100599.
- [15] C. W. Li, J. Hong, A. F. May, D. Bansal, S. Chi, T. Hong, G. B, 2009, 80, 125203. Ehlers, O., Delaire, *Nat. Phys.*, 2015, **11**, 1063-1069.
- [16] Y. Zhu, B. Wei, J. Liu, N. Z. Koocher, Y. Li, L. Hu, W. He, G. Deng, W. Xu, X. Wang, *Mater. Today Phys.*, 2021, **19**, 100428.
- [17] B. Wei, Q. Sun, C. Li, J. Hong, Sci. China Phys. Mech. Astron., 2021, 64, 1-34.
- [18] N. K. Ravichandran, D. Broido, *Phys. Rev. B*, 2018, **98**, 85205.
- [19] T. Feng, X. Ruan, Nanoscale Energy Transp., 2020, 2-1.
- [20] Y. Shen, C. N. Saunders, C. M. Bernal, D. L. Abernathy, M. E. Manley, B., Fultz, *Phys. Rev. Lett.*, 2020, **125**, 085504.
- [21] C. McGuire, K. Sawchuk, A., Kavner, J. Appl. Phys., 2018, **124**, 115902.
- [22] Y. Zhang, J. Dong, P. R. Kent, J. Yang, C. Chen, *Phys. Rev.* 4, 958-965. **B**, 2015, **92**, 20301.
- [23] G. A., Slack, J. Phys. Chem. Solids, 1973, 34, 321-335.
- [24] L. Lindsay, D. Broido, T. Reinecke, *Phys. Rev. Lett.*, 2013, 111, 25901.
- 165201.
- **361**, 575-578.

- [27] A. Kundu, X. Yang, J. Ma, T. Feng, J. Carrete, X. Ruan, G. K. Madsen, W. Li, *Phys. Rev. Lett.*, 2021, **126**, 115901.
- [28] W. G. Zeier, A. Zevalkink, Z. M. Gibbs, G. Hautier, M. G. Kanatzidis, G. J. Snyder, Angew. Chem. Int. Edit., 2016, 55, 6826-6841.
- [29] J. Moore, R. Williams, R. Graves, *Phys. Rev. B*, 1975, 11, 3107.
- [30] https://www.crystran.co.uk/optical-materials.
- [31] Z. Zhang, Y. Guo, M. Bescond, J. Chen, Nomura, M. S., Volz, Phys. Rev. B. 2021, 103, 184307.
- [3] R. Reddy, K. R. Gopal, K. Narasimhulu, L. Reddy, K. R. [32] Z. Zhang, Y. Guo, M. Bescond, J. Chen, S. Nomura, Volz, Phys. Rev. Lett., 2022, 128, 15901.
 - [33] P. E. Blöchl, *Phys. Rev. B*, 1994, **50**, 17953.
 - [34] G. Kresse, J. Hafner, *Phys. Rev. B*, 1993, **47**, 558.
 - [35] G. Kresse, J. Hafner, *Phys. Rev. B*, 1994, **49**, 14251.

 - [37] Hongzhiwei Technology, Device Studio, Version 2021A, Available 2021. online: https://iresearch.net.cn/ cloudSoftware.
 - [38] S. Maintz, V. L. Deringer, A. L. Tchougréeff, R., Dronskowski, LOBSTER: A tool to extract chemical bonding from plane-wave based DFT. Wiley Online Library: 2016.
 - [39] T. A. Manz, N. G., Limas, *RSC Adv.*, 2016, **6**, 47771-47801.
 - [40] N. G. Limas, T. A. Manz, *RSC Adv.*, 2016, **6**, 45727-45747.
 - [41] N. G. Limas, T. A. Manz, *RSC Adv.*, 2018, **8**, 2678-2707.
 - [42] A. Togo, F. Oba, I., Tanaka, *Phys. Rev. B*, 2008, **78**, 134106.
 - [43] W. Li, J. Carrete, N. A. Katcho, N., Mingo, *Comput. Phys. Commun.*, 2014, **185**, 1747-1758.
 - [44] S. Baroni, S. De Gironcoli, A. Dal Corso, P. Giannozzi, Rev. Mod. Phys., 2001, 73, 515.
 - [45] W. Mei, L. Boyer, M. Mehl, M. Ossowski, H., Stokes, *Phys.*
 - [46] A. Ward, D. Broido, D. A. Stewart, G., Deinzer, Phys. Rev.
 - [47] G. Raunio, L. Almqvist, R., Stedman, *Phys. Rev.*, 1969, **178**,
 - [48] J. Reid, T. Smith, W., Buyers, *Phys. Rev. B*, 1970, **1**, 1833.
 - [49] J. Copley, R. Macpherson, T. Timusk, *Phys. Rev.*, 1969, **182**, 965-972.
 - [50] A. Woods, W. Cochran, B. Brockhouse, *Phys. Rev.*, 1960, **119**, 980-999.
 - [51] G. Dolling, R. Cowley, C. Schittenhelm, I. Thorson, *Phys. Rev.*, 1966, **147**, 577-582.
 - [52] G. Raunio, S. Rolandson, J. Phys. C: Solid State Phys., 1970, **3**, 1013.
 - [53] S. Rolandson, G. Raunio, J. Phys. C: Solid State Phys., 1971,
 - [54] G. Raunio, S. Rolandson, *Phys. Status Solidi B*, 1970, 40, 749-757.
 - [55] A. Ahmad, H. Smith, N. Wakabayashi, M. Wilkinson, *Phys. Rev. B*, 1972, **6**, 3956.
- [25] L. Lindsay, D. Broido, T., Reinecke, *Phys. Rev. B*, 2013, **87**, [56] J. F. Vetelino, K. Namjoshi, S. Mitra, *Phys. Rev. B*, 1973, **7**,
- [26] J. S. Kang, M. Li, H. Wu, H. Nguyen, Y., Hu, *Science*, 2018, [57] H. Liu, C. Yang, B. Wei, L. Jin, A. Alatas, A. Said, S. Tongay, F. Yang, A. Javey, J. Hong, *Adv. Sci.*, 2020, 7, 1902071.

Research article ES Energy & Environment

[58] C. Li, N. K. Ravichandran, L. Lindsay, D. Broido, *Phys. Rev.* Lett. 2018, 121, 175901.

[59] W. Ren, Y. Ouyang, P. Jiang, C. Yu, J. He, J., Chen, Nano *Lett.*, 2021, **21**, 2634-2641.

Author Information



Zheng Chang is a Ph.D. candidate in the University of Technology, China. His doctoral supervisor is Associate Prof. Xiaoliang Zhang. His research is mainly

focused on the theoretical study of the lattice thermal and electrical transport properties in thermoelectric materials with first-principles calculations and ab initio molecular dynamics simulations.



Bin Wei is an assistant professor in the School of Materials Technology at Henan Polytechnic University and currently a postdoctoral Engineering at Tsinghua University in

Prof. Jiawang Hong in Mechanics from the School of mechanism under extreme conditions. Aerospace Engineering from Beijing Institute of Technology, China in 2020. He was a short-term scholar with Assistant Prof. Chen Li in the Department of Mechanical Engineering at University of California, Riverside, USA in 2019. His research interests include lattice dynamics, inelastic neutron/X-ray scattering, and thermoelectric materials.



Xiaoliang Zhang is associate an professor in Dalian University of Technology. He received his PhD degree in Engineering Thermophysics from Chinese Academy of Sciences in 2013. He was a joint PhD student in Laboratory of *Thermodynamics* in **Emerging** Technologies at ETH Zurich between

2010 and 2011. He was a research engineer in Department of Chemical and Biomolecular Engineering at National University of Singapore between 2012 and 2013. After PhD graduation, he worked as a postdoctoral researcher at RWTH Aachen University between 2013 and 2016. His research is mainly focused on molecular dynamics simulations and firstprinciples calculations of nanoscale thermal transport.



Ming Hu received the B.S. degree from Department of Mechanical Engineering, University of Science and Technology of China in 2001 and the Ph.D. degree in solid mechanics from Institute of Mechanics, Chinese Academy of Sciences in 2006. He is currently a faculty member Department of Mechanical

Key Laboratory of Ocean Energy Engineering, the University of South Carolina. His research Utilization and Energy Conservation of interests include thermal transport in novel energy systems, Ministry of Education and School of interfacial heat transfer for thermal management, and Energy and Power Engineering at Dalian artificial intelligence accelerated advanced materials discovery.



Dawei Tang received his B.S., M.S., and Ph.D. degrees at Jilin University (1985), Institute of Metal Research, Chinese Academy of Sciences (1988), and Shizuoka University in Japan (1999), respectively. After 10-years of faculty at Shizuoka University (1993-2004), he

Science and joined the Institute of Engineering Thermophysics, Chinese Academy of Sciences, and served as a professor and director of Heat and Mass Transfer Research Center. Since 2016, he research fellow with Prof. Yuanhua Lin in joined Dalian University of Technology as a professor and the the School of Materials Science and dean of School of Energy and Power Engineering. His research interests include evaluation on thermophysical China. He received his Ph.D. degree under the supervision of properties of new functional materials, and energy transport

> Publisher's Note: Engineered Science Publisher remains neutral with regard to jurisdictional claims in published maps and institutional affiliations.